ARTICLE

Observation of Excited $\nu_\mathrm{s}(\mathrm{NO_2})$ and Relaxation Process of HNS in Solution by CARS Technique

Gen-bai Chu[a], Min Shui[a], Yun-fei Song[b], Tao Xu[c*], Yu-qiu Gu[a*], Yan-qiang Yang[b]

a. Science and technology on Plasma Physics Laboratory, Research Center of Laser Fusion, China Academy of Engineering Physics, Mianyang 621900, China
b. Department of Physics, Harbin Institute of Technology, Harbin 150001, China
c. Institute of Chemical Materials, China Academy of Engineering Physics, Mianyang 621900, China

Investigation on vibrational excitation and relaxation process will provide important information for a better understanding of ultrafast dynamic response of energetic materials. Using sub-ps time-resolved coherent anti-Stokes Raman scattering (CARS) experiments, we directly observe excitation of vibrational mode $\nu_\mathrm{s}(\mathrm{NO_2})$ and its relaxation process of ground state HNS (2,2′,4,4′,6,6′-hexanitrostillbenein) in solution. The results show that $\nu_\mathrm{s}(\mathrm{NO_2})$ at 1385 cm^{-1} has been excited and relaxation time of 0.38 and 8.5 ps is obtained. The possible quantum beat frequencies are also discussed via fs-CARS experiments. The original results provide an insight into ultrafast process of energetic materials.

Key words: 2,2′,4,4′,6,6′-Hexanitrostillbene, Vibrational mode, Coherent anti-Stokes Raman scattering

I. INTRODUCTION

It is an ultrafast dynamic response of energetic material molecules to a number of different ignition processes, such as photons, sparks or shocks [1, 2]. Yet on the molecular level, it is very little known about how the ignition energy from an impact couples into molecules. Excited states played a crucial role in the energy conversion of energetic materials and have been extensively investigated [2−6]. The local heating effect called "hot spot" is previously thought to be induced by fast non-radiative transition of excited states, which also accelerate the chain reactions of energetic materials. Recently, smaller and colder hot spot has been created by long-wavelength infrared radiation (28−30 THz), providing direct evidence in violation of "hot spot" via fast non-radiative transition of excited states [7]. In addition, the fragmentation of 2,2′,4,4′,6,6′-hexanitrostillbene (HNS, Fig.1) has been observed at irradiation of long wavelength of 1024 nm [8]. The phenomena make researchers rethink about how the initiation energy couples into molecules. In this sense, vibrational relaxation of initially excited mode and the flow of vibrational energy into low frequency continuum of energetic materials should be performed in the UV or infrared range [9]. It is noted that ultraviolet laser may excite energetic material molecules to excited electronic states, which will decompose on electronic excited potential surface [2].
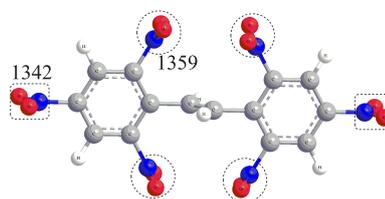

FIG. 1 Geometrical structure of HNS molecule.

In the UV or infrared range, fundamental ultrafast motions including molecular vibrations and rotations characterize the chemical bonding and determine the reactions dynamics [10]. The timescales for these motions are typically 100 fs for vibrations and 100 ps for rotations, respectively. Vibrationally hot ground electronic states have been recognized as an important factor in the energy transfer process of photochromic molecules. And the rotational dynamics accessed on S_0 or excited electronic potential surface may be quenched by intermolecular steric hindrance with the increase of nitro group in energetic materials [11]. In different kinds of ultrafast pump-probe techniques, sub-ps or fs time-resolved coherent anti-Stokes Raman scattering (CARS) technique is a powerful tool to study high-frequency vibrational modes with high spectral resolution, and it has been widely employed in liquid phase and gas phase materials [10, 12−16]. The functional NO_2 group of HNS studied by CARS technique is very significant [4].

Nevertheless, due to the nonresonant part of susceptibility, the disadvantage of CARS technique limits de-

—————
*Authors to whom correspondence should be addressed. E-mail: xuzhtao@126.com, yqgu@caep.ac.cn

tection ∼1% for aqueous solution or opaque material [17]. It is noted that the energetic material HNS is hardly dissolved into solution and its crystal is light yellow, which limits the utilization of CARS technique for trace HNS or other explosive study. The evolution of vibrational characteristics of liquid energetic materials such as CH_3NO_2, $C_6H_5NO_2$ *etc.* have been observed [2, 18−21]. The evolution of excited state of HNS has also been observed by the ultrafast absorption experiments [22]. The thermal decomposition of HNS has been analyzed by Fourier transform infrared spectroscopy (FTIR) and differential scanning calorimetry (DSC) [20]. The continuing effort will be performed on HNS with sub-ps and fs-CARS technique.

In this work, sub-ps and fs-CARS experiments are utilized to observe excitation of vibration and its relaxation process of HNS in solution. The results show that $\nu_s(NO_2)$ at 1385 cm^{-1} has been excited and the relaxation time of 0.38 and 8.5 ps is obtained by sub-ps-CARS. The possible quantum beat frequencies are also discussed via fs-CARS experiments. The original results provide an insight into the ultrafast process of HNS.

II. EXPERIMENTS

The schematic diagram of CARS experimental setup [23] is shown in Fig.2 and the measurements are performed at room temperature. The laser pulses are generated from a regenerative amplifier (1 kHz, Spectra-Physics, Spitfire) with center wavelength of 800 nm, single pulse energy of 500 μJ, pulse duration of 130 fs, and they are split into three parts. In sub-ps-CARS experiments, the first two are stretched by a grating, pass through a slit of 3 mm width and then are compressed by another grating, after which, pulse duration of 500 fs and spectral resolution of 3.6 nm (47 cm^{-1}) are obtained. In fs-CARS experiments, no slit or grating is used, where pulse duration of 130 fs and spectral resolution of 10 nm (150 cm^{-1}) are obtained. The two pulses are used as the pump and probe pulses, respectively. The third one is collimated on 1 mm thick H_2O to produce a white-light continuum (WLC), which is used as the Stokes pulse. Two delay lines are employed, where the Stokes pulse defines an arbitrary temporal zero point. In this way, different delay time between the pump and Stokes pulse and that between the probe and Stokes pulse can be achieved. A folded Box-CARS configuration with properly chosen angles (less than 2°) between the beams, determined by the phase matching condition, is used. The CARS signal is collected by a silica fiber, dispersed in a spectrometer (Bruker Optics 500 IS/SM) and detected by a CCD detector (Andor DU440-BU2).

The sample is first subjected to two time-coincident pump and Stokes pulses. If the frequency difference of the two pulses matches the frequency of a specific vi-
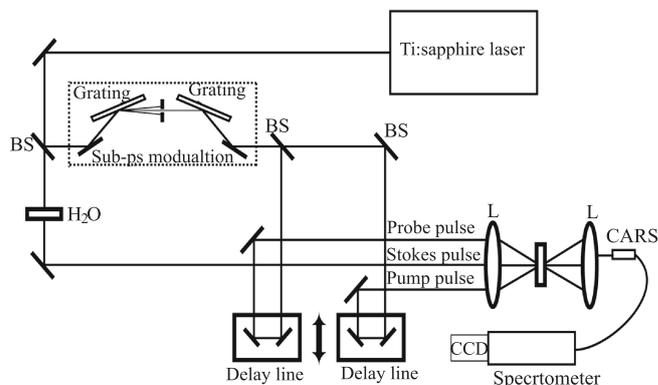

FIG. 2 Experimental setup of the CARS technique. BS: beam splitter, L: lens.

brational mode, this mode will be excited coherently. The temporal evolution of the coherent vibrations is probed by the third time-delayed probe pulse, giving rise to a CARS signal. The signal intensity is recorded as a function of the time delay between the probe pulse and the simultaneous pump and Stokes pulses. In this work, we use a WLC for the Stokes pulse, which has an ultra-broadband spectral profile ranging from 400 nm to 1100 nm. In order to suppress the excitation of other modes and the generation of the degenerate four-wave mixing process, the WLC is spectrally filtered using a filter to cut off the components of wavelength less than 830 nm. Due to the chirp characteristics of the ultra-broadband WLC, no complicated laser system is required for the wavelength tuning of the Stokes pulse. The pump, Stokes, and probe pulses are focused on the samples to a diameter of about 300 μm using a lens with a focal length of 300 mm. The length of the spatial overlap of all the three laser beams is about 10 mm and can cover well the thickness of the samples (1 mm). The single pulse energies at the sample are 1−10 μJ for the pump and probe pulses, and 1 μJ for the Stokes pulse, respectively. The polarization of the three pulses is set to be parallel to each other. The temporal overlap between the pump and Stokes pulses is properly adjusted to accomplish selective excitation of appointed vibrational modes.

The low-frequency vibration modes ranging up to 1000 cm^{-1} are submerged in a fast intense nonresonant part due to the electronic system. In sub-ps-CARS experiments, the CARS at one time delay are selected for clarification, in which only the high frequency vibration modes are shown in the work. The sub-ps resolved spectra are obtained with the typical step of 50 fs and maximum time delay of 10 ps, covering the overall relaxation process. In the fs resolved spectra, a typical step of 25 fs and maximum time delay of 5 ps are adopted.

HNS (with a purity >99.5%) used in the experiments is synthesized at Institute of Chemical Materials, China Academy of Engineering Physics. The synthesis of HNS is a two-step reaction, first oxidative cou-
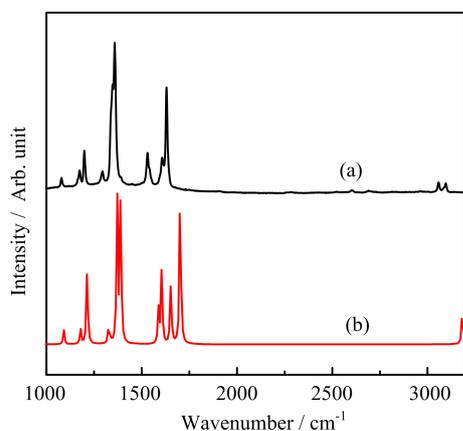
FIG. 3 (a) Experimental and (b) calculated Raman spectra of HNS.

TABLE I Vibrational mode and IR frequency (cm^{-1}) of experimental and calculated HNS as well as CH$_3$CN.

Mode	HNS		CH$_3$CN	Intensity
	Expt.	Theor.		
δ(C6−H)	1199	1213		m
δ(C=C−H)	1295	1289		w/vw
ν_s(NO$_2$)	1342	1371		s
δ(C−H)			1374	vw
ν_s(NO$_2$)	1359	1390		s
ν_{as}(NO$_2$)	1531	1588		m
ν_{as}(NO$_2$)	1607	1604		m
ν(C6=C6)	1630	1653		m
ν(C=C)		1702		s
ν(C−H)			2941	s
ν(=C−H)	3058	3182		m
ν(C6−H)	3096	3233		m

pling of trinitrotoluene (TNT), and then dehydration and recrystallization. In the experiments, HNS powder is dissolved into CH$_3$CN with the concentration of 2 mmol/L (HNS in (CH$_3$)$_2$SO (DMSO) with concentration of 1 mmol/L, the results are shown in supplementary material). The Raman spectrum of HNS in solid state is shown in Fig.3(a). The geometrical structure and frequency calculations are performed at the B3LYP/6-311G(d,p) level by using Gaussian 09 suite of programs [24], and the calculated Raman spectrum result is shown in Fig.3(b).

III. RESULTS AND DISCUSSION

The strong peaks at 1342 and 1359 cm^{-1} in Raman spectrum of HNS are consistent with 1371 and 1390 cm^{-1} in calculated Raman spectrum in Table I, respectively. Both of them are assigned to ν_s(NO$_2$) at different positions in HNS molecule, as shown in Fig.1,

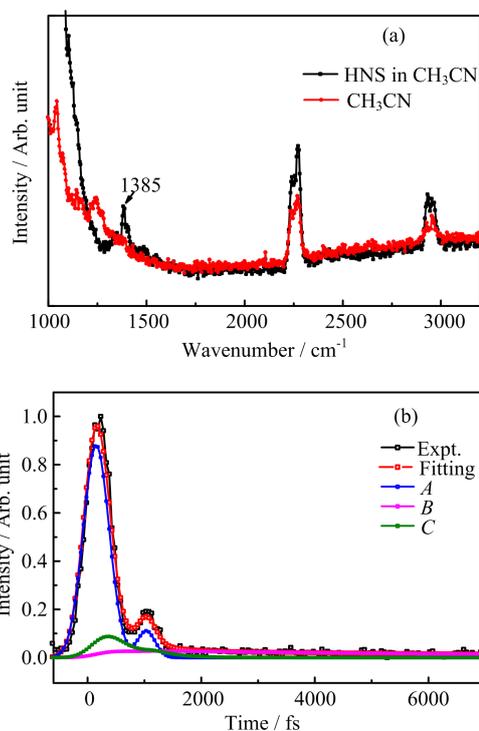FIG. 4 (a) CARS of HNS in CH$_3$CN at time delay of 1 ps and (b) relaxation process of ν_s(NO$_2$) as well as fitting curves. A, B, C show the fitting curves referring to the three coefficients in Eq.(1).

respectively. The corresponding vibrations are also observed in FTIR spectrum with high intensity [20]. But the relatively low concentration of HNS in CH$_3$CN leads to nearly no observable intensity of HNS Raman signal in Fig.S1 (supplementary material). By utilization of coherent excitation at wavelength of 800−1100 nm and non-background detection, CARS signal is 10^4−10^6 times sensitive than that of Raman spectrum and solvent effect is greatly reduced [17]. Since CARS is a superior tool for obtaining spectra of certain solutes in solution, observation of HNS in CH$_3$CN by CARS technique is feasible.

In order to illuminate the vibrations of HNS in CH$_3$CN, sub-ps-CARS at time delay of 1 ps are selected for clarification and shown in Fig.4. The peak at 1385 cm^{-1} is attributed to signal of HNS. The two peaks of 1342 and 1359 cm^{-1} in Raman spectrum could not be distinguished in CARS at spectral resolution of 47 cm^{-1}. Nevertheless, the δ_s(CH$_3$) mode of CH$_3$CN at 1374 cm^{-1} in Fig.S1 may influence the observation of the ν_s(NO$_2$) of HNS. Thus, we carefully check CH$_3$CN CARS with and without HNS at different time delays, identify the influence is neglectable and safely assume that the peak at 1385 cm^{-1} is from HNS. In addition, a vibration at 1385 cm^{-1} for HNS in DMSO is also observed in Fig.S2 (supplementary material), further confirming 1385 cm^{-1} band arises from HNS. The vibrational relaxation is extracted as a function of peak in-

tensity *vs.* time delay, and it lasts for ∼6 ps in Fig.4(b). The signal shows expected exponential decays for the high density of coherent excited normal modes in the ground state of this system. The difference of the vibration relaxation from response function fulfills the Eq.(1) as follows:

$$I_s(t) = \left[A\delta(t) + B\exp\left(\frac{-t}{T_1}\right) + C\exp\left(\frac{-t}{T_2}\right) \right]^* G(t) \quad (1)$$

where $I_s(t)$, A (B, C), T_1 (T_2), *, and $G(t)$ refer to the dynamic CARS signal, coefficient, relaxation time, convolution, and response function, respectively. The different components of three parts are shown in Fig.4(b). The decay times T_1 and T_2 of 0.38±0.05 and 8.5±1 ps are extracted from the best fit of the curve, respectively.

After initial excitation at 800 nm or longer wavelength, HNS molecule populates a virtual state or vibrationally excited state. Such state may be unobservable. By the coherent pump and Stokes pulses with frequency difference matches, a high frequency vibrational $\nu_s(NO_2)$ mode at 1385 cm^{-1} could be excited and observed. This vibration corresponds to the symmetric vibration of crucial NO_2 group in energetic materials. The vibration can provide energy to the molecule, break bonds by overcoming a reaction coordinate barrier, and lead to different chemistry (*e.g.* NO_2 release). This point is in good agreement with slow heating effect on energetic materials. It is noted that the initially vibrational excitation decays through pathways that involve the excitation of one or more vibrations of the solute or solvent, and one or more excitations of the low frequency continuum of the medium [9, 25]. The continuum is composed of the instantaneous normal modes in a liquid. While in a mixed crystal sample, the low frequency continuum is composed of the well-defined acoustic and optical phonons of the crystal. The fragmentation of HNS at irradiation of 1024 nm may result from this particular energy transfer from initially excited vibration to low frequency phonons in solid sample [8]. The smaller and colder hot spot created by long-wavelength infrared radiation may also provide evidence for this explanation [7]. In this sense, the insight into vibrational excitation will provide important information for a better understanding of thermal, shock-induced and photon-induced chemistry of energetic materials [26].

The vibrational relaxation pathways of high excited C≡N stretching modes have been studied by ultrafast back-electron transfer [27]. The time scale of the first excited vibrational state is typically 0.8 ps for intramolecular vibrational redistribution (IVR) and 20 ps for intermolecular vibrational energy relaxation (VER), respectively. The latter is close to the vibrational cooling dynamics of azobenzene in vibrationally hot ground electronic state which has been determined to be on a time scale of ca. 20 ps via time-resolved IR spectroscopy with femtosecond time resolution [28]. In this paper, we obtain relaxation times of 0.38 and 8.5 ps,
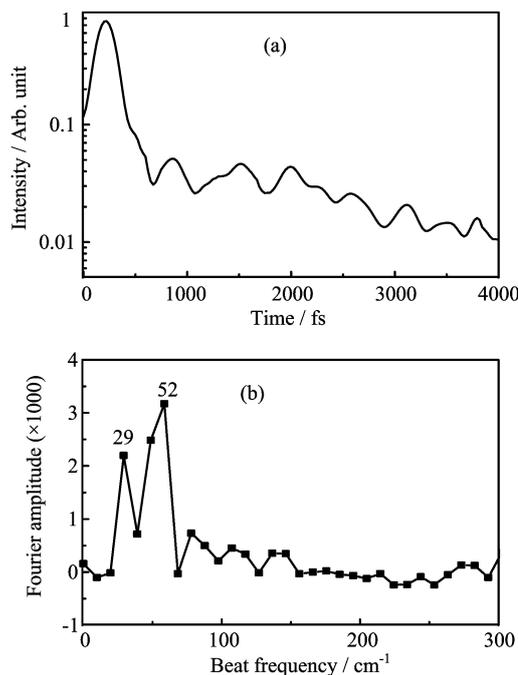

FIG. 5 (a) Time evolution of wavenumber 1350 cm^{-1} and (b) Fourier transform of frequency slices at 1350 cm^{-1} of HNS in CH$_3$CN.

which can be attributed to IVR and VER processes, respectively. The former one obtained from experiments is the dephasing time (T_{dec}), which consists of energy relaxation (T_{er}) and pure dephasing (T_{dec}^*) contribution. The overall value for vibrational dephasing rate is described as a sum of the anharmonic decay rate and the pure dephasing rate,

$$\frac{1}{T_{\text{dec}}} = \frac{1}{T_{\text{er}}} + \frac{1}{T_{\text{dec}}^*} \quad (2)$$

It is difficult to distinguish the contribution of the two processes. T_{er} for IVR process of $\nu_s(NO_2)$ is longer than 0.38 ps, in agreement with IVR rate of 0.6 ps for β-carotene [29] and 0.8 ps for C≡N stretching modes [27]. The solute-solvent interaction has little effect on IVR process [29]. The timescale of 8.5 ps for VER process of $\nu_s(NO_2)$ is much shorter than 20 ps for C≡N stretching modes [27] and azobenzene [28]. It is uncertain that such process may be accelerated by strong steric hindrance of HNS. Further effort should be made to more explicit and accurate investigation on low or high excited vibrational states of energetic materials.

In fs-CARS experiments, different vibrational modes could be excited simultaneously at one pulse wavelength because of large spectral bandwidth of fs laser pulses. The quantum beat phenomena of two excited vibrations may be observed in the experiments. We analyze the fs-CARS signals at wavenumber of 1350 cm^{-1} starting from time delay of 500 fs in Fig.5, to avoid intense nonresonant contribution. These beats frequencies are

determined by Fourier transform, following subtraction of the exponentially decaying backbond associated with this w_{CARS} signal. In comparison with the known Raman active frequency of the ground state HNS, it is straightforward using the dispersed time resolved CARS to assign all of the observed beat frequencies to pairs of known vibrational modes. Two major beat frequencies at 29 and 52 cm^{-1} are evident from this spectrally integrated signal. Four Raman active modes are known to be present in this region with frequencies of 1294, 1342, 1359 and 1530 cm^{-1}, thus 29 cm^{-1} beat is assigned to coherence of 1342 and 1359 cm^{-1}. The 52 cm^{-1} beat is readily assigned to coherence of 1342 and 1294 cm^{-1} vibrational mode.

IV. CONCLUSION

In this work, sub-ps and fs CARS experiments have been performed to observe the excitation of vibrational mode and its relaxation process of HNS in solution. Sub-ps CARS experiments have better spectral resolution and we directly observe the excitation of vibrational mode $\nu_s(NO_2)$ at 1385 cm^{-1} by this method. By changing the time delay between pump and probe beams, two relaxation times of 0.38 and 8.5 ps are obtained for the vibrational mode. The relaxation times are related with the intramolecular vibrational redistribution and intermolecular vibrational energy relaxation, respectively. The results are favorable with the fragmentation of HNS at irradiation of 1024 nm and colder hot spot created by long-wavelength infrared radiation. In fs CARS experiments, different vibrational modes could be excited simultaneously at one pulse wavelength. We observe the oscillation compound by changing pump-probe time delay, which could be attributed to beat frequencies. Two major beat frequencies at 29 and 52 cm^{-1} are assigned to coherence of 1342−1359 cm^{-1} and 1342−1294 cm^{-1} vibrational mode, respectively. The original results provide an insight to the ultrafast response of HNS and a better understanding of thermal, shock-induced and photon-induced chemistry of energetic materials.

Supplementary material: Raman spectra of HNS in CH$_3$CN, sub-ps CARS of HNS in DMSO, and fs-CARS of CH$_3$CN are shown.

V. ACKNOWLEDGMENTS

[1] S. Odiot, J. Phys. Colloq. **48**, 225 (1987).

[2] C. Rajchenbach, G. Jonusauskas, and C. Rulliere, J. Phys. IV **5**, 365 (1995).

[3] A. Bhattacharya and E. R. Bernstein, J. Phys. Chem. A **115**, 4135 (2011).

[4] A. Bhattacharya, Y. Guo, and E. R. Bernstein, J. Chem. Phys. **136**, 024321 (2012).

[5] Z. Yu and E. R. Bernstein, J. Chem. Phys. **137**, 114303 (2012).

[6] Z. Yu and E. R. Bernstein, J. Phys. Chem. A **117**, 1756 (2013).

[7] M. W. Chen, S. You, K. S. Suslick, and D. D. Dlott, Appl. Phys. Lett. **104**, 061907 (2014).

[8] Y. Sun, T. Xu, Y. J. Shu, X. Wang, Z. Q. Zhao, and Y. Q. Gu, Asian J. Chem. **25**, 4247 (2013).

[9] V. M. Kenkre, A. Tokmakoff, and M. D. Fayer, J. Chem. Phys. **101**, 10618 (1994).

[10] T. C. W. Kiefer, M. Heid, A. Materny, M. Schmitt, T. Siebert, and A. Vierheilig, Proc. SPIE 4749 (2002).

[11] N. Tamai and H. Miyasaka, Chem. Rev. **100**, 1875 (2000).

[12] M. Schmitt, G. Knopp, A. Materny, and W. Kiefer, Chem. Phys. Lett. **270**, 9 (1997).

[13] O. Rubner, M. Schmitt, G. Knopp, A. Materny, W. Kiefer, and V. Engel, J. Phys. Chem. A **102**, 9734 (1998).

[14] M. Schmitt, G. Knopp, A. Materny, and W. Kiefer, J. Phys. Chem. A **102**, 4059 (1998).

[15] C. L. Evans and X. S. Xie, Annu. Rev. Anal. Chem. **1**, 883 (2008).

[16] A. Materny, J. Konradi, V. Namboodiri, M. Namboodiri, A. Scaria, V. K. Vaidyan, and V. S. Jayakumar, AIP Conf. Proc. 43 (2008).

[17] W. M. Tolles, J. R. Mcdonald, and A. B. Harvey, Appl. Spectro. **31**, 253 (1977).

[18] A. A. Zenin and S. V. Finjakov, Combustion, Explosion, and Shock Waves **45**, 559 (2009).

[19] J. S. Lee, C. K. Hsu, and C. L. Chang, Thermochimica Acta **392**, 173 (2002).

[20] G. d. Silva, K. Iha, A. M. Cardoso, E. C. Mattos, and R. d. C. L. Dutra, J. Aero. Techno. Manag. **2**, 41 (2010).

[21] B. C. Pein, Y. Sun, and D. D. Dlott, J. Phys. Chem. A **117**, 6066 (2013).

[22] G. B. Chu, Y. Xiong, J. Yi, K. M. Cheng, T. Xu, J. T. Xin, and Y. Q. Gu, RSC Advances (in press), DOI:10.1039/c4ra08305a.

[23] X. Du, M. Zhang, Q. Meng, Y. Song, X. He, Y. Yang, and J. Han, Opt. Exp. **18**, 22937 (2010).

[24] H. Okamoto and K. Yoshihara, Chem. Phys. Lett. **177**, 568 (1991).

[25] H. Fujisaki and J. E. Straub, Proc. Natl. Acad. Sci. **102**, 6726 (2005).

[26] I. V. Adamovich, S. O. Marcheret, J. W. Rich, and C. E. Treanor, AIAA J. **33**, 1064 (1995).

[27] M. S. Lynch, K. M. Slenkamp, and M. Khalil, J. Chem. Phys. **136**, 241101 (2012).

[28] P. Hamm, S. M. Ohline, and W. Zinth, J. Chem. Phys. **106**, 519 (1997).

[29] K. Y. Hiromi Okamoto, Chem. Phys. Lett. **177**, 568 (1991).